The Journal of Experimental Biology **198**, 1637–1646 (1995)
Printed in Great Britain © The Company of Biologists Limited 1995

OPTICAL SCALING IN CONSPECIFIC *CATAGLYPHIS* ANTS

CHRISTOPH P. E. ZOLLIKOFER[1,*], RÜDIGER WEHNER[1] AND TSUKASA FUKUSHI[2]
[1]*Zoologisches Institut, Universität Zürich-Irchel, Winterthurerstrasse 190, CH-8057 Zürich, Switzerland* and
[2]*Miyagi College of Education, Department of Biology, Aoba-Yama, Sendai 980, Japan*

Accepted 18 April 1995

Summary

This study examines the effects of body size variation on the optical properties of the compound eyes of visually guided desert ants belonging to the genus *Cataglyphis*. Although linear head size may vary by a factor of 2 within conspecific workers and most optical parameters change accordingly, the extent of the visual field remains constant. Comparative measurements carried out on workers of three species (*C. albicans*, *C. bicolor* and *C. fortis*) and on reproductive females and males of one species (*C. bicolor*) show that the form (size and shape) of the visual field is highly characteristic for each caste/species. A constant visual field is realised by reciprocal scaling rules for the number of ommatidia and the angular spacing of ommatidia. While larger ants have more ommatidia per compound eye, interommatidial angles are reduced accordingly, thus giving rise to a constant visual field. Among conspecific ant workers, the relationship between spatial visual acuity and eye size is similar to that found in interspecific comparisons and reflects optical constraints imposed on the design of the compound eye. Mapping of spatial visual directions onto the compound eye surface reveals a characteristic, inhomogeneous distribution of interommatidial spacing, particularly a foveal band with increased visual acuity in the vertical direction. This 'visual stretch' viewing the horizon is similar to that found in a variety of flying insects. Although, among conspecific workers, both the number of ommatidia and the interommatidial angles vary with varying head size, the overall pattern of interommatidial spacing is maintained so that corresponding positions on the compound eye of small and large individuals look in equivalent directions in space. These findings are in accordance with the observation that the shape of the compound eye surface, as expressed by the radius of curvature along cross sections, is similar in small and large ants.

Key words: ants, body size, *Cataglyphis*, compound eye, divergence angles, Formicidae, optics, pseudopupil, scaling.

Introduction

Even though the worker castes of most ant genera, including the Old World desert ants of the genus *Cataglyphis*, are monomorphic (Hölldobler and Wilson, 1990; Wehner, 1983), individual workers of a given species come in various sizes. In *Cataglyphis*, they may vary by a factor of 2 in linear dimensions (e.g. head width; *C. albicans*, 0.8–1.7 mm; *C. bicolor*, 1.5–3.2 mm; Wehner, 1983). Furthermore, the workers of all *Cataglyphis* species are highly visually guided navigators, not relying on pheromone trails while foraging, so how do differently sized workers compare in their visual performances? First and foremost, how do the optics of the ants' compound eyes (e.g. optical parameters such as the size of the visual field, the angular distance between adjacent ommatidia, the radius of curvature of the eye, etc.) scale with the size of the animal?

There are likely to be trade-offs between particular optical functions. For example, take the simple observation that, within conspecific individuals, eye size decreases with decreasing body size. Small ants have fewer and smaller ommatidia than large ants. Does this mean that small ants exhibit lower visual acuities or smaller fields of view than larger ants? In other words, is field size functionally more important than acuity, or *vice versa*? Answers to such questions might reveal some important functional aspects of the ant's visually guided behaviour. They might also shed some light on the developmental constraints of compound eye design, because the size and the shape of the eye are governed by some basic developmental rules. As shown by Franks and Norris (1987) for the ant genera *Atta*, *Eciton* and *Pheidole*, allometric relationships of varying pairs of body measurements are linked over the entire body.

In the latter context, one should recall that ants, like all hymenopterans, are holometabolous insects, which pass through a complete metamorphosis. Consequently, their

*Address for correspondence: Institut für Informatik, MultiMedia Laboratorium, Universität Zürich-Irchel, Winterthurerstrasse 190, CH-8057 Zürich, Switzerland.

postembryonic life cycle consists of several larval stages, a pupal stage and one final stage, the imago. As only the imago (in this case the worker ant) possesses compound eyes and as the imago does not grow, body size and, hence, eye size remain constant during the life span of an individual ant. However, the shape of the size-frequency distribution of the workers can be controlled by the colony (most probably by differential larval feeding). It varies according to season and/or the amount of forage available in the habitat (R. Wehner, unpublished observations obtained from several *Cataglyphis* species). As a consequence, the relative number of workers belonging to a particular size class and, hence, exhibiting particular optical properties of their eyes varies during the course of the year. This observation might add further interest to our study.

Materials and methods

Species

Live individuals of *Cataglyphis bicolor* Fabr. (workers, reproductive females, and males; for species rank, see Wehner *et al.* 1994) and live workers of *C. albicans* Santschi and *C. fortis* Forel were taken from colonies in Maharès (Tunisia: 34.58 ˚ N, 10.50 ˚ E) and reared in the laboratory. Linear size varied by a factor of 2 within conspecific workers.

Measurement of optical axes of ommatidia

The spatial directions of the optical axes of ommatidia were determined by examining corneal as well as deep pseudopupils under antidromic illumination conditions (Franceschini, 1975; Via, 1977). The head of an ant was glued onto the tip of a light guide (diameter 1 mm) and mounted in the centre of a goniometer (Fig. 1). The outer axis (β) of the goniometer was adjusted along a plane perpendicular to the optical axis of the microscope. Then, under the microscope, the head of the ant was adjusted so that its sagittal plane was parallel to the equatorial plane of the goniometer. Assuming this position, the poles of the spherical coordinate system of the goniometer were aligned with the laterally looking ommatidia of the left and right compound eyes. By rotating the goniometer about its poles (Fig. 1, axis λ), the head was rotated on its transversal axis and adjusted according to the position assumed during free walking. This position was defined by an angle of 45 ˚ between the horizon and the rear margin of the compound eye. Using this experimental arrangement, two different types of measurement were performed; first, the spatial direction of the optical axis of single ommatidia in a spherical coordinate system was determined [(λ,β); for definitions and conventions see Table 1] and, second, individual ommatidia oriented in a pre-defined direction (λ,β) in space were identified. In the latter case, it was necessary to locate the position of the respective ommatidia on the surface of the compound eye. To this end, minute quantities of optical grinding powder (silicon carbide particles) were dispersed over the compound eyes to serve as landmarks. During optical measurements, the position of any given ommatidium was defined relative to several conspicuous landmarks in its neighbourhood. Since the particles maintained their original position during scanning electron microscopy, they could be used for subsequent identification of the absolute position of ommatidia on the compound eye.

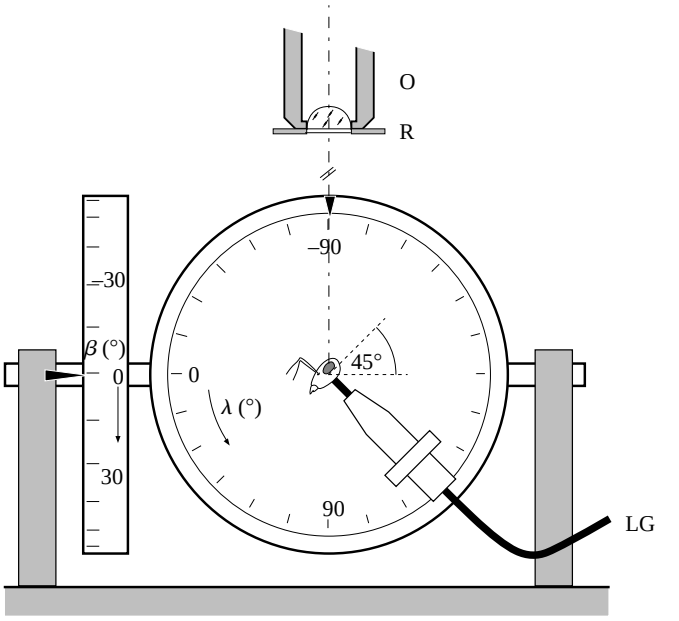

Fig. 1. Experimental arrangement. The head of an ant was glued onto the tip of a light guide (LG, used for antidromic illumination) and positioned in the centre of a goniometer such that its sagittal plane was at 90 ˚ to axis λ. The rear margin of the compound eye was adjusted to give an angle of 45 ˚ with axis β, corresponding to the position of the head during free walking. A microscope was used to observe the deep pseudopupil of the compound eye. The spatial direction of the optical axis of any ommatidium can be determined by turning along axes λ and β and aligning the deep pseudopupil with the optical axis of the microscope (O). A ring of white paper (R) glued around the front lens of the microscope was used for determination of corneal normal axes under orthodromic illumination conditions (see Materials and methods).

A compound eye system of coordinates was defined on the basis of the ommatidial rows: After counting the *x*-, *y*- and *z*-rows, the respective median rows were marked. The ommatidium nearest to the intersection point of the three rows defined the origin of the coordinate system. Ommatidial positions could then be expressed in (*x*,*y*,*z*)-coordinates of the hexagonal raster grid by counting rows from the origin. The *x*-axis of this system of coordinates is equivalent to the vertical axis (*V*) of the *HV*-system proposed by Stavenga (1979). In order to facilitate comparisons among eyes of different sizes, coordinates (*x*,*y*,*z*) were normalised to a range between −1.0 and +1.0 [(x',y',z'), see Fig. 4].

Visual field

The boundaries of the visual field of compound eyes were determined by measuring the spatial directions of the optical axes of the marginal ommatidia. To this end, the goniometer

Table 1. *List of variables*

Variables describing optical properties of the compound eye	
A_φ	Area of a hexagonal tile on the unit sphere, centred around the optical axis of an ommatidium (steradian, sr) (see Fig. 2)
(α,ϵ)	Spherical coordinate system of the environment with north being the zenith ($\epsilon = 90°$)
(λ,β)	Spherical coordinate system with north being the left lateral point of the ant's field of view ($\alpha = 90°$, $\epsilon = 0°$)
$\Delta\varphi_{x,y,z}$	Divergence angle (degrees) between optical axes of neighbouring ommatidia, measured along ommatidial *x*-, *y*- and *z*-rows, respectively
$\Delta\varphi$	Average of the values of $\Delta\varphi_{x,y,z}$ at a given ommatidial position (degrees)
F, L, R, Z	Frontal, left, right and zenithal directions
T	Area of a triangle subtended on the unit sphere by three adjacent ommatidial positions (sr)
U	Area of the unit sphere (4π sr)
V_t	Total area of visual field of one compound eye (percentage of unit sphere)
V_b	Area of binocular overlap of one compound eye (percentage of unit sphere)
V_o	Blind region of one compound eye (percentage of unit sphere)
Variables describing morphometric properties of the compound eye	
A_c	Area of the surface of the compound eye (mm^2)
A_c'	Area of the compound eye projected onto a plane through its margins (mm^2)
A_o	Area of one ommatidial lens (mm^2)
D_{15}	Distance between two points on the surface of the compound eye whose corneal surface normals include an angle of 15° (mm)
D_{75}	Distance between two points on the surface of the compound eye whose corneal surface normals include an angle of 75° (mm)
D_o	Diameter of an ommatidial corneal lens (mm)
H_c	Height of the compound eye, measured perpendicular to ommatidial *z*-rows (mm)
k	Factor scaling D_o with $\sqrt{R_c}$ in diffraction-limited compound eyes (Kirschfeld, 1976)
N_o	Number of ommatidia in one compound eye
R_c	Radius of curvature of the compound eye (mm)
W_c	Width of the compound eye, measured along ommatidial *z*-rows (mm)
W_h	Head width (mm)
(x,y,z)	Hexagonal coordinate system of the ommatidial rows of a compound eye
(x',y',z')	Normalised hexagonal coordinate system

was rotated about the axis λ (corresponding to a rotation about the transversal axis of the ant's head) at fixed intervals of 10° (Fig. 1, angle λ). At each position of λ, the goniometer was tilted about its outer axis (Fig. 1, angle β) until the pseudopupil of a marginal ommatidium was centred. This position indicated the alignment of the optical axis of an individual ommatidium with that of the microscope. The angular deviation β from the sagittal plane (β=0°) was then read to the nearest 0.5°.

Subsequently, the distribution of the optical axes across the compound eye of worker ants was analysed. At each position of a spherical coordinate grid (λ=0°, 15°,..., 270°; β=−15°, 0°, 15°,..., 90°), the ommatidium whose optical axis was aligned with the microscope axis was identified. Using landmarks on the eye surface, as described above, every grid point (λ,β) could be identified on scanning electron micrographs of the compound eye and transformed to (x',y',z')-coordinates.

For the sake of clarity, measurements performed in the spherical coordinate system of the goniometer (λ,β) were transformed to geographical coordinates corresponding to the natural position of the head during walking (azimuth α and elevation ϵ; frontal direction α=0°, ϵ=0°; lateral: α=±90°, ϵ=0°; zenith: ϵ=90°; see Fig. 3A).

By projecting the boundaries of the visual field of a compound eye onto a unit sphere, it was possible to quantify the area of the whole visual field (V_t) and, by reference to the sagittal plane, the area of binocular overlap (V_b) as well as the area not accessible to vision (blind area, V_o) (see Table 1). With U denoting the area of the unit sphere, the following equation holds true:

$$U = 2(V_t - V_b + V_o) = 4\pi. \quad (1)$$

Determination of divergence angles

The spatial orientation of individual ommatidial axes was determined in the frontal (α=0°; ϵ=0°), lateral (α=90°; ϵ=0°) and caudal (α=150°; ϵ=0°) regions of the eye. In each region, optical axes were determined according to the following protocols: the ommatidium with its optical axis closest to one of the directions mentioned above was selected as a centre point. Tracking along the *x*-, *y*- and *z*-rows outwards from the centre yielded a starlike pattern of 12 ommatidial axis positions (Fig. 2). Divergence angles ($\Delta\varphi$) between any two ommatidial axes (α_1,ϵ_1) and (α_2,ϵ_2) were calculated using the following formula:

$$\cos\Delta\varphi = \sin\epsilon_1\sin\epsilon_2 + \cos\epsilon_1\cos\epsilon_2\cos(\alpha_2 - \alpha_1). \quad (2)$$

According to the directions given by ommatidial rows, interommatidial angles were grouped in categories $\Delta\varphi_x$, $\Delta\varphi_y$ and $\Delta\varphi_z$. To obtain a direction-independent measure of interommatidial angles, the parameter A_φ (divergence area) was defined to denote the area that can be attributed to each ommatidium when covering the unit sphere with hexagonal tiles centred on ommatidial axes (Fig. 2). A_φ can be calculated as follows: let T denote the area of a triangle subtended on the unit sphere by three adjacent ommatidial positions (Fig. 2),

$$T = \arccos[(\cos\Delta\varphi_x - \cos\Delta\varphi_y\cos\Delta\varphi_z)/(\sin\Delta\varphi_y\sin\Delta\varphi_z)] + \arccos[(\cos\Delta\varphi_y - \cos\Delta\varphi_x\cos\Delta\varphi_z)/(\sin\Delta\varphi_x\sin\Delta\varphi_z)] + \arccos[(\cos\Delta\varphi_z - \cos\Delta\varphi_x\cos\Delta\varphi_y)/(\sin\Delta\varphi_x\sin\Delta\varphi_y)]. \quad (3)$$

For small values of $\Delta\varphi_{x,y,z}$,

$$A_\varphi = 2T. \quad (4)$$

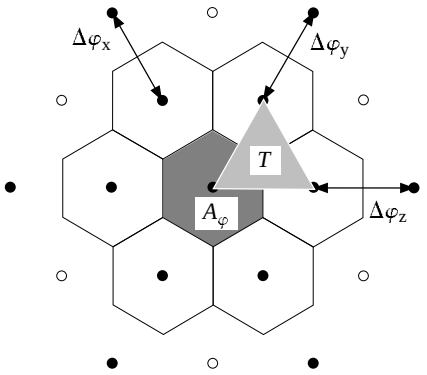

Fig. 2. Definition and measurement of optical parameters of the compound eye. A small area of the unit sphere is projected onto the drawing plane. Filled circles indicate positions of the optical axes of ommatidia determined using the deep pseudopupil method, open circles indicate interpolated values for intercalating ommatidia. Divergence angles between the optical axes of adjacent ommatidia (i.e. distances on the unit sphere, $\Delta\varphi_{x,y,z}$) are measured along ommatidial rows (*x*, *y* and *z*, respectively). The divergence area A_φ is a direction-independent measure of the spatial packing density of ommatidia and is represented by a hexagonal tile attributed to each ommatidium. For small values of $\Delta\varphi$, A_φ equals twice the area of a triangle (*T*) subtended between the optical axes of adjacent ommatidia.

Determination of morphometric parameters

Preliminary studies showed that all marginal ommatidia of one compound eye lie close to one plane, whose orientation is defined by a normal vector where $\alpha=\pm65^\circ$, $\epsilon=60^\circ$ for the left and right eyes, respectively. Scanning electron micrographs of both compound eyes of 24 *C. bicolor* workers were taken from this position and used to measure the area (A_c'), height (H_c) and width (W_c) of the eyes. A_c' represents a two-dimensional estimate of the convex corneal surface area (A_c).

Determination of the radius of curvature of the corneal surface

Since every corneal facet is individually convex, the cornea of the compound eye as a whole does not appear as a smooth surface, which would be a prerequisite for determination of the radius of curvature. However, an accurate description of the corneal surface of the compound eye can be provided in the form of a grid, consisting of the midpoints of all ommatidial corneal facets and the normals to the surface at each point of the grid. Using optical methods, it was possible to determine the midpoint of the corneal facets as well as the normal to the surface of each midpoint (referred to as the *ommatidial surface normal*).

To this end, a ring of white paper was glued around the aperture of the front lens of the microscope (Fig. 1). Under diffuse illumination, the cornea of each ommatidium acts as a convex mirror surface reflecting the dark microscope aperture surrounded by the bright ring. The mirror image is perfectly centred in the corneal facet whose ommatidial surface normal is aligned with the microscope axis (with increasing divergence between these two axes, the image becomes more off-centred). At any given goniometer position, the ommatidium displaying a centred mirror image of the ring indicates the position of the local centre of curvature and, correspondingly, of the normal to the surface of the compound eye (referred to as the *corneal surface normal*). Using this method, photomicrographs were taken along the lateral meridian, from the dorsal to the ventral rim of the eye; ($\alpha=90^\circ$) at intervals of $\Delta\epsilon=15^\circ$. On each photomicrograph, the position of the corneal surface normal was determined, and linear distances between successive positions (D_{15}) were measured. Five successive values of D_{15} were summed to obtain the length of the whole section (D_{75}). The local radius of curvature (R_c) between two positions of corneal surface normals was estimated by:

$$R_c = D_{15}/(2\sin7.5^\circ). \quad (5)$$

Following procedures analogous to those described for mapping ommatidial axes, the spatial directions of the corneal surface normals were mapped onto the surface of the compound eye.

Results

Extent of the visual field

The spatial extent of the visual field of the compound eyes was determined in workers, reproductive females and males of *Cataglyphis bicolor* and in workers of *C. fortis* and *C. albicans* (Fig. 3). As a general feature, visual fields exhibit a region of binocular overlap with frontal/dorsal orientation and attaining maximum lateral extent near the zenith (Fig. 3A,B). Posteriorly as well as below the horizon, there is an optically inaccessible area (blind region). When projected onto a unit sphere, the spatial extent of the visual field approximates that of a laterally oriented hemisphere which is slightly inclined towards the contralateral side in the region of the zenith.

To study the influence of head size on the properties of the visual field, data were sampled from workers with head widths varying by a factor of 2 in each of the species mentioned above. Data from individual *C. bicolor* workers (Fig. 3B,C) show that neither the overall size nor the shape of the visual field varies with increasing head width. Analogous observations could be made in *C. fortis* and *C. albicans*, indicating that the form (size and shape) of the visual field as a whole is held constant among conspecific workers. In each species, however, the form of the visual field exhibits characteristic traits, notably with respect to lateral extent and the proportions of the binocular and blind regions. For example, *C. fortis* exhibits a marked zenithal constriction of the binocular region, whereas *C. albicans* shows an extended blind region.

In a further step, sex-related differences were studied in *C. bicolor*. Measurements performed on reproductive females indicate that the dimensions of the visual field do not differ from those found in workers of the same species (Fig. 3B). In males, pseudopupil measurements were hampered by intense internal pigmentation of the compound eye. Nevertheless, data

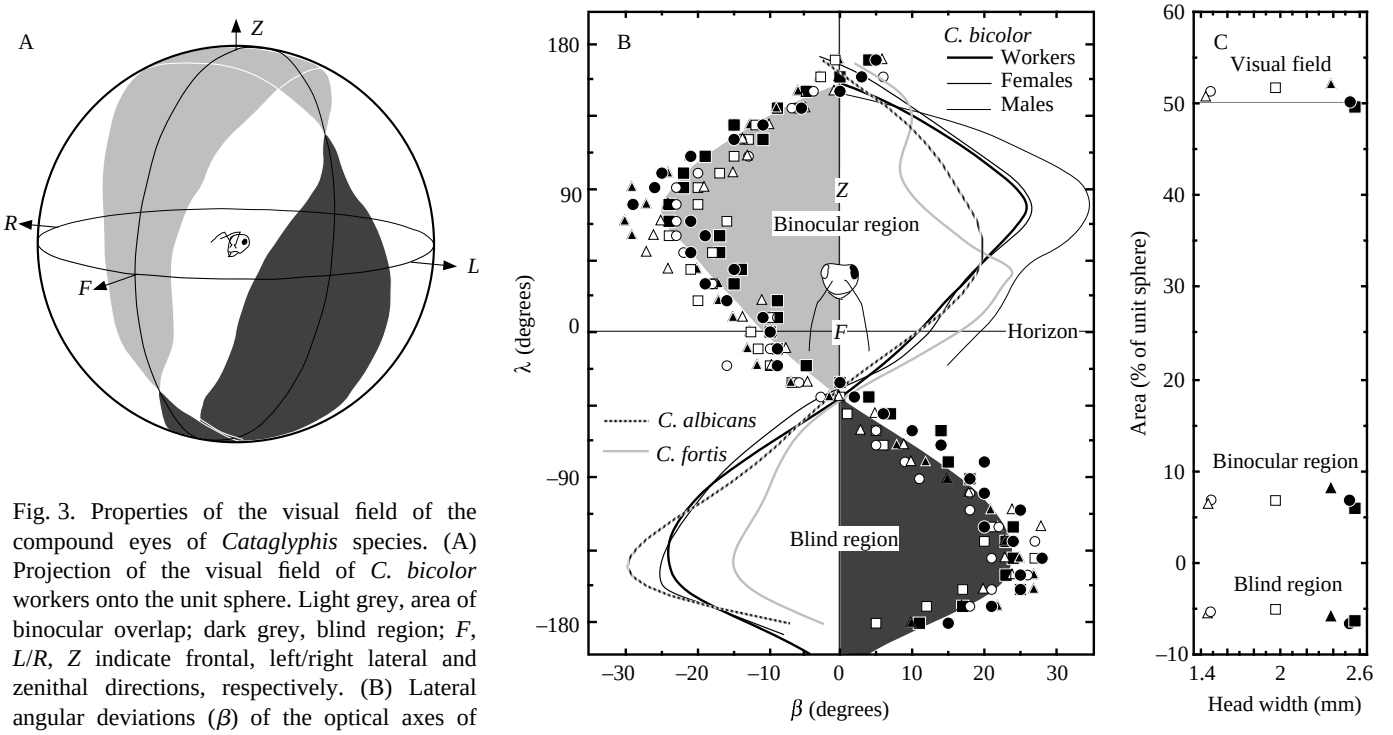

Fig. 3. Properties of the visual field of the compound eyes of *Cataglyphis* species. (A) Projection of the visual field of *C. bicolor* workers onto the unit sphere. Light grey, area of binocular overlap; dark grey, blind region; *F*, *L*/*R*, *Z* indicate frontal, left/right lateral and zenithal directions, respectively. (B) Lateral angular deviations (β) of the optical axes of marginal ommatidia from the midplane of the head (β=0°); left eye, data for six *C. bicolor* workers of different sizes [head width (mm): filled squares 2.56, filled circles 2.53, filled triangles 2.39, open squares 1.96, open circles 1.47, open triangles 1.45]; right eye, average boundaries calculated for workers, reproductive females (*N*=2) and males (*N*=2) of *C. bicolor* (solid lines; note differences between workers/females and males) and for workers of *C. fortis* (*N*=6) and *C. albicans* (*N*=6) (broken lines). (C) Area of the visual field *versus* head width in workers of *C. bicolor* (same individuals and symbols as in B). Areas are expressed as a percentage of the surface area of a unit sphere (4π sr; 100 %); the horizontal line indicates the size of a hemisphere (2π sr; 50 %). The sizes of the different regions of the visual field do not depend on head width.

from two individuals clearly indicate that males differ from females with respect to the size and shape of the region of binocular overlap (Fig. 3B). We can thus state that the overall form of the visual field exhibits species-specific as well as sex-specific features, but does not vary with varying head size.

Properties of the visual field

Further analyses of the properties of the visual field were carried out on workers of *Cataglyphis bicolor*. To record the overall distribution of the spatial orientation of the optical ommatidial axes, a 30°×30° azimuth/elevation grid of spatial directions (α,ϵ) was back-projected onto the compound eye. This was achieved by identifying the ommatidia whose optical axes were oriented in the directions of the grid points. To facilitate comparisons among individuals, ommatidial positions on the compound eye were expressed in normalised hexagonal coordinates [(x',y',z'); see Materials and methods]. Projection of a given spatial direction (α,ϵ) onto the surface of the compound eye always yielded the same surface position (x',y',z'), irrespective of the head width of the individual under examination. It was thus possible to pool the data obtained from 10 workers and to compute average values.

The spatial distribution of the ommatidial axes on the surface of the compound eye exhibits regional as well as directional asymmetries (Fig. 4A). The distances between the horizontal grid lines (which are at equal vertical angular distances of $\Delta\epsilon$=30°) indicate that the regions above and below the horizon (between ϵ=±30°) are over-represented and appear to be vertically expanded compared with adjacent regions (from ϵ=+30° to +60°, and from ϵ=−30° to −60°). Further, it is evident that the spacing of the vertical grid lines (with horizontal angular distance $\Delta\alpha$=30°) is consistently smaller than that of the horizontal grid lines. This means that the compound eye exhibits a pronounced horizontal/vertical astigmatism. Examination of the distribution of the divergence angles $\Delta\varphi_x$ (measured along the vertically oriented ommatidial *x*-rows) reveals a foveal belt of elevated vertical resolution, especially in the frontal and caudal regions of the compound eye (Fig. 4B).

Scaling of optical parameters

It emerges as an overall result from the above analyses that, for conspecific workers of different sizes, the extent of the visual field is constant and corresponding regions on the compound eye point to corresponding spatial directions in space. At the same time, however, morphometric features of the compound eye, for example the number of ommatidia, are known to increase with increasing head width (Menzel and Wehner, 1970). Consequently, one might expect that interommatidial angles would decrease with increasing head

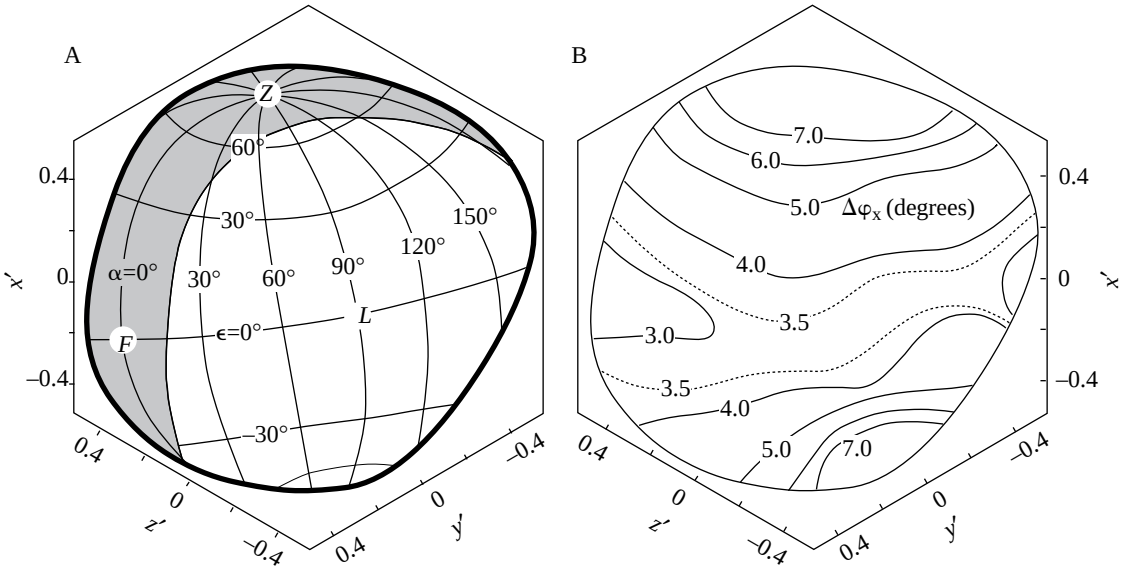

Fig. 4. (A) Projection of the visual space (azimuth, α; elevation, ϵ) onto the left compound eye of a *Cataglyphis bicolor* worker [pooled data from 10 individuals; axes x', y' and z' indicate a normalised system of coordinates, described in Materials and methods; row numbers range between 36 and 39 (x), 37 and 45 (y), 38 and 46 (z)]; (α,ϵ) grids are at intervals of 30°; *F*, *L* and *Z* indicate frontal, left lateral and zenithal directions, respectively; grey area, region of binocular overlap. (B) Distribution of divergence angles $\Delta\varphi_x$ (degrees) between ommatidial optical axes, measured along *x*-rows. The distribution shows a pronounced 'foveal belt' along the horizon (data for a medium-sized *C. bicolor*; head width 2.01 mm; 940 ommatidia).

Table 2. *Coefficients of log–linear regression equations relating different variables to head width*

Dependent variable (range)	Exponent *a*	Factor *b*	r^2	*N*	*P*
Optical variables					
V_t (6.26–6.56 sr)	–0.02±0.03	0.81	0.13	6	0.49
A_φ frontal (0.0022–0.0100 sr)	–0.84±0.44	–1.98	0.17	20	<0.01
A_φ lateral (0.0035–0.0140 sr)	–0.72±0.06	–2.00	0.27	206	<0.01
A_φ dorsal (0.0057–0.0190 sr)	–0.65±0.13	–1.70	0.43	37	<0.01
$\Delta\varphi$ lateral (3.71–5.07°)	–0.31±0.05	0.71	0.50	19	<0.01
$\Delta\varphi$ dorsal (5.21–6.69°)	–0.48±0.05	0.92	0.98	4	<0.02
Morphological variables					
A_c' (0.091–0.452 mm^2)	1.68±0.07	–1.12	0.96	48	<0.01
H_c (0.39–1.01 mm)	0.93±0.05	-0.48	0.89	48	<0.01
W_c (0.28–0.62 mm)	0.80±0.05	-0.56	0.87	48	<0.01
D_{75} (0.29–0.66 mm)	1.10±0.14	0.67	0.99	4	<0.02
D_o (0.0135–0.0200 mm)	0.50±0.03	–1.88	0.98	6	<0.01
N_o (743–1254)	0.74±0.08	2.81	0.85	19	<0.01
R_c (0.140–0.636 mm)	0.96±0.16	–0.78	0.58	30	<0.01

Coefficients are given for log–linear equations of the form $\log_{10}(\text{variable}) = a\log_{10}(W_h)+b$, where head width ($W_h$) ranges between 1.28 and 2.70 mm.

Values of $\Delta\varphi$ are mean values for individual ants.

Data for N_o and D_o are from Menzel and Wehner (1970).

Explanations of the variables are given in Table 1.

Values for *a* are given as means ± S.E.M.

dimensions. To confirm this, divergence angles ($\Delta\varphi$) were measured in individuals of different sizes. Data sampling was confined to three areas positioned along the horizon (i.e. in the region of highest vertical resolution), at α=0° (frontal), α=90° (lateral) and α=150° (caudal). Despite considerable variation within and between individuals, it is obvious that divergence angles decrease with increasing head width (Fig. 5A). With respect to spatial direction, $\Delta\varphi_x$ is consistently smaller than $\Delta\varphi_y$ and $\Delta\varphi_z$, providing direct evidence for the foveal belt along the horizon (Fig. 4B). In

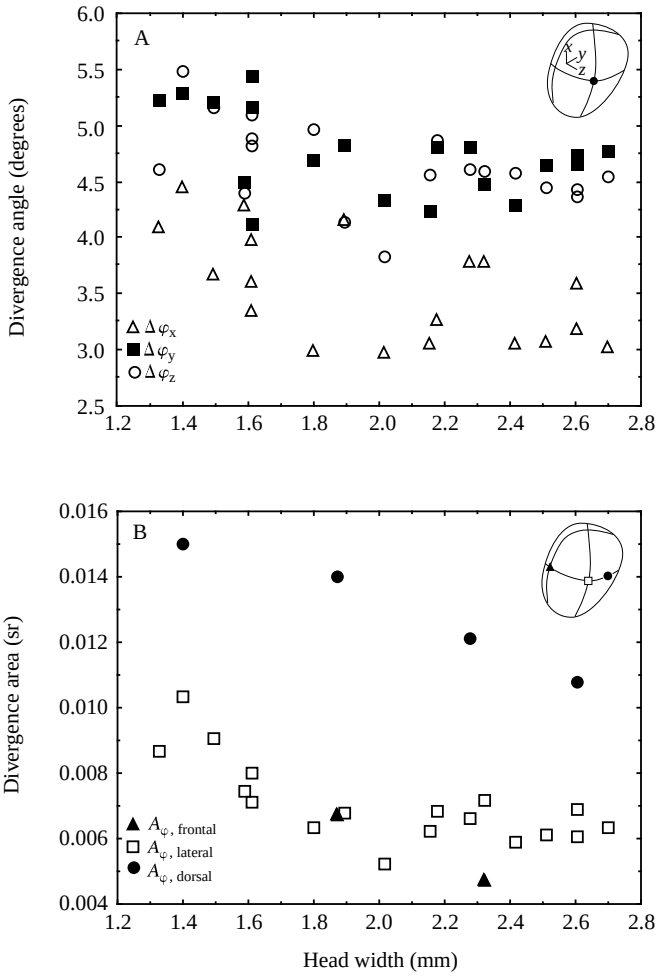

Fig. 5. Optical scanning density in *Cataglyphis bicolor* workers of different sizes. (A) Plot of divergence angles $\Delta\varphi_x$, $\Delta\varphi_y$, $\Delta\varphi_z$ (degrees) *versus* head width (mm); data for the lateral sampling region. (B) Plot of divergence areas A_φ (sr) *versus* head width; data for frontal, lateral and dorsal regions.

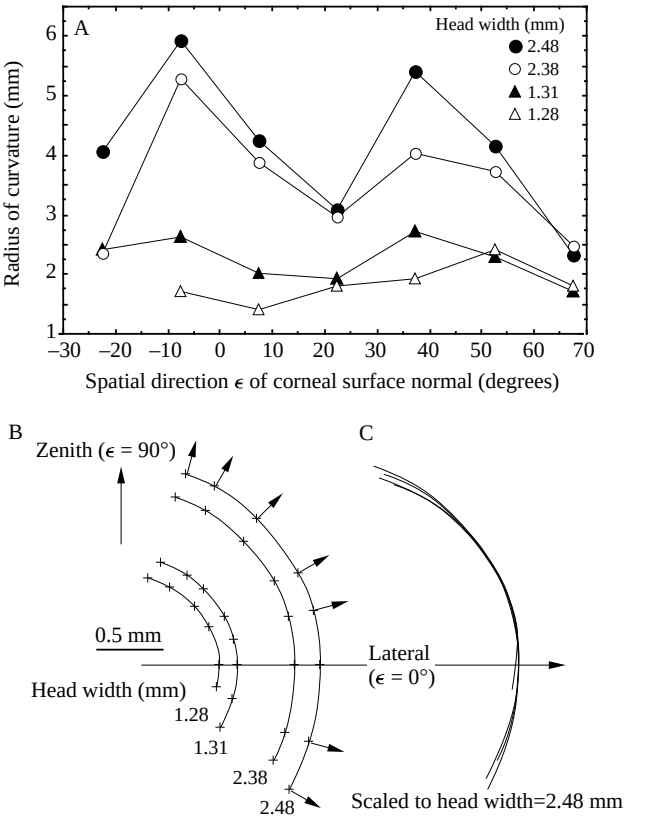

Fig. 6. Geometric properties of the surface of the compound eye of four workers of *Cataglyphis bicolor*. (A) Distribution of the radius of curvature (R_c) along a section through the lateral meridian (azimuth α=90°, from elevations ϵ=−22.5° to ϵ=67.5°). (B) Reconstruction of the cross section through the compound eye; crosses indicate points of measurement of the corneal surface normal (arrows; see Materials and methods). (C) The superposition of the cross sections scaled to the same relative size shows nearly isometric scaling of the compound eye in this region (see Table 2).

order to obtain direction-independent data and to reduce the individual variation, mean values of ommatidial divergence areas (A_φ, see Materials and methods and Fig. 2) were calculated for the frontal, lateral and dorsal sampling areas (Fig. 5B). As with $\Delta\varphi$, divergence areas A_φ (sr) decrease with increasing head width. Log–linear regression equations (Table 2) show that, with increasing head width, both A_φ (average exponent −0.70) and $\Delta\varphi$ (average exponent −0.39) decrease significantly.

Scaling of morphometric parameters

Now that the optical parameters of the compound eye have been related to head size, it is necessary to complete the analysis by examining the scaling properties of the underlying morphological features of the eye. The surface area (A_c'), height (H_c) and width (W_c) of compound eyes were measured on scanning electron micrographs. In relation to head width (W_h), A_c' scales with an exponent less than 2, and the exponents of height and of width of the compound eye differ from each other (Table 2). This signifies that compound eyes change their relative size and form as head size varies. The radius of curvature (R_c) of the surface of the compound eye was measured along an optical cross section taken through the lateral meridian (α=90°; see Materials and methods). Data from four worker ants with different head widths show consistent fluctuations of R_c along the section (Fig. 6A). Peaks of R_c near the horizon (ϵ=0°) as well as at medium elevation (ϵ=45°) indicate flattening of the surface in these regions. The conspicuous interindividual similarity of the data can be expressed in quantitative terms. Both the mean radius of curvature along the section (R_c, Table 2) and the length of the surface segment under examination (D_{75}, Table 2) scale with head width with an exponent near 1. Accordingly, reconstructions of the cross sections that had been rescaled to the same relative size (Fig. 6C), show geometric similarity between individuals of different sizes.

Discussion

The variability of body size in conspecific workers of *Cataglyphis* ants is of considerable significance with respect to the ecological consequences for the species as a whole (Wehner *et al.* 1972) as well as for the behaviour of individual ants (Zollikofer, 1994). Since workers of *Cataglyphis* species are individual foragers that rely mainly on visual cues for homing (see review by Wehner, 1992), a comparative examination of the visual system in small and large ants is of special interest. Scaling properties of the visual system similar to those described in this study reflect developmental constraints imposed on the morphological design of the compound eye and determine its optical performance. These intraspecific data can then be compared with the interspecific scaling properties of the compound eyes of insects in general. Since the latter have been shown to reflect adaptation to optical performance constraints (see Wehner, 1981), it is of special interest to compare intra- and interspecific variation with respect to different constraints acting on the morphogenesis and phylogenesis of the compound eye.

Among conspecific *Cataglyphis* workers, the visual field of compound eyes is shown to be independent of head size. This is a unique feature, especially if one bears in mind that virtually every other dimension of the compound eye depends on head size, which itself varies by a factor of 2. With the evidence presented in this study, for *Cataglyphis bicolor* workers, it is possible to demonstrate that visual field constancy is an effect of the exact tuning of morphological and optical scaling rules governing eye growth.

Our measurements showed that the estimated (planar) area of the compound eye scales to head width (W_h) as:

$$A_c' \propto W_h^{1.68}. \quad (6)$$

As the area A_c' is roughly proportional to the height (H_c) multiplied by the width (W_c) of the compound eye, we can explain the above exponent by combining the respective scaling exponents:

$$A_c' \propto H_c W_c \propto W_h^{0.93} W_h^{0.80} \propto W_h^{1.73}. \quad (7)$$

Since A_c' scales with an exponent smaller than 2, relative eye size decreases with increasing head size, giving the eyes of larger individuals a smaller appearance. Moreover, since there are scaling differences between height and width, the compound eyes assume a more elliptical shape in larger individuals. Earlier measurements concerning the number and size of ommatidia (recalculated from Menzel and Wehner, 1970) showed that large compound eyes contain more and larger ommatidia than small ones. Ommatidial size (A_o, surface area) scales isometrically with head width, whereas the number of ommatidia (N_o) increases more slowly:

$$A_o \propto D_o^2 \propto W_h^{1.00}, \quad (8)$$

$$N_o \propto W_h^{0.74}. \quad (9)$$

If we combine these two equations, we can estimate the relationship between head width and the surface of the compound eye (A_c),

$$A_c = N_o A_o \propto W_h^{0.74+1.00} \propto W_h^{1.74}. \quad (10)$$

This prediction is in good agreement with our measurements for A_c' (see equation 6). We will now turn our attention to optical scaling properties. Given the above values for increased ommatidial numbers in large individuals, visual field constancy can only be achieved by reducing interommatidial angular distances. In fact, the spacing between the optical axes of adjacent ommatidia, whether measured by divergence angles ($\Delta\varphi_x$, $\Delta\varphi_y$, $\Delta\varphi_z$) or by areas on the unit sphere (A_φ), becomes smaller with increasing head width:

$$\Delta\varphi \propto W_h^{-0.39}, \quad (11)$$

$$A_\varphi \propto W_h^{-0.70}. \quad (12)$$

Because $\Delta\varphi$ represents a distance on the unit sphere, whereas A_φ represents an area, the ratio of the exponents of equations 11 and 12 is approximately 1:2. It follows from the definition of A_φ (Fig. 2) that the total visual field of one compound eye (V_t) can be expressed as the sum of the areas A_φ of all ommatidia,

$$V_t = N_o A_\varphi. \quad (13)$$

Hence, by combining equations 9 and 13, we find for the following relationship between the visual field and head width:

$$V = N_o A_\varphi \propto W_h^{0.74-0.70} \propto W_h^{0.04} \approx \text{constant}. \quad (14)$$

We can therefore state that, because of opposite allometric scaling coefficients for the number of ommatidia (0.74) and for the interommatidial spacing (-0.70), the total visual area of a compound eye remains constant. Moreover, taking into account that the form of the visual field is distinctive in each species and, as shown for *C. bicolor*, in conspecific males and females, it appears that this character is of great functional significance. Species-specificity and sex-specificity of visual fields have been described in a wide range of insects and have been extensively discussed with respect to behavioural implications such as predation and mating (see Horridge, 1978; Land, 1989; Stavenga, 1992). In *Cataglyphis* foragers, behavioural and physiological studies showed that the extent and form of the binocular region (notably its dorsal rim area) are of major importance for polarised light orientation (Wehner, 1994). The observed differences between the visual fields of males and females of *C. bicolor* may reflect diverse behavioural adaptations. Since our knowledge about the mating behaviour of *C. bicolor* is still anecdotal (it can be studied only during a 3 week period each year; R. Wehner and S. Wehner, unpublished observations), we can only speculate that the extent of the binocular area in males might be related to this behavioural context.

What are the optical implications of a constant-sized visual field? Among conspecific worker ants, a constant visual field and a decreasing number of ommatidia lead to poorer visual acuity (i.e. increased values of $\Delta\varphi$) in smaller individuals. Negative correlation of eye size and visual acuity is a well-

known phenomenon and can be traced to optical limitations and constraints imposed on the design of compound eyes. As has been demonstrated several times (Barlow, 1952; Kirschfeld, 1976; Snyder, 1979), diffraction-limited compound eyes demonstrate a characteristic relationship between the diameter of a corneal facet (D_o) and the radius of curvature of the corneal surface (R_c),

$$D_o = k\sqrt{R_c} = kR_c^{0.5};\ k \approx 0.5\,. \quad (15)$$

Taking into account additional limitations imposed on the design of a compound eye (photon signal-to-noise ratio; Snyder, 1979), especially in fast-moving insects, the actual values of D_o are expected to exceed those given in equation 15. For an extended range of insect species, it appears as a rule that D_o is at least twice as large as expected (Wehner, 1981):

$$D_o \approx 2kR_c^{0.5} = R_c^{0.5}\,. \quad (16)$$

It is now possible to establish an equivalent relationship for our sample of conspecific worker ants. Combining the equations for D_o and R_c (Table 2) yields:

$$D_o = 0.9R_c^{0.52}\,. \quad (17)$$

When comparing equations 16 and 17, one has to take into account that the former is derived from interspecific variation, whereas the latter describes intraspecific variation. Further, it is reasonable to assume that size-related intraspecific variation primarily reflects developmental constraints, whereas interspecific variation depicts adaptation to environmental constraints. Thus, the apparent similarity of equations 16 and 17 shows that the optical constraints imposed on the design of compound eyes are fundamental to both morphogenetic and phylogenetic processes.

In our sample of conspecific workers, head widths vary by a factor of 2, and visual acuity (which is inversely proportional to both $\Delta\varphi$ and A_φ) varies by a factor of $2^{0.70}$=1.62. How do smaller ants cope with this apparent loss of visual acuity, since one might expect that errors made in reading the points of the celestial compass will increase correspondingly? From behavioural studies, we know that in comparing *C. albicans* and *C. bicolor*, foraging distance is roughly proportional to the size of the forager (Wehner, 1987). Hence, we may conclude that, in small individuals, orientation errors are compensated for by shorter foraging distances. However, the compound eye of ants is a multifunctional visual organ with regionally distinct morphological and physiological properties and functions (Fent, 1985; Wehner, 1991).

If we consider the inhomogeneous spacing of the optical axes (Fig. 4), it appears that the resulting acuity gradients may be more significant than absolute visual acuity. This view is supported by the fact that gradients and astigmatism of $\Delta\varphi$ similar to those described here have already been reported in a variety of flying insects (see review by Land, 1989). For example, foveal belts along the horizon representing a vertical acuity gradient have been reported in bees (Baumgärtner, 1928; Horridge, 1978), wasps (Horridge, 1978), butterflies (del Portillo, 1936) and locusts (Autrum and Wiedemann, 1962; Land, 1981, p. 555) and may be involved in functions such as maintaining horizontal head position or tracking distant landmarks on the horizon. Taking into account that the species reported are of different sizes, one is led to the conclusion that, in performing such tasks, gradient information is more important than absolute resolving power. Further, the fact that *Cataglyphis* ants walking on the ground exhibit optical gradient patterns almost identical to those found in flying insects may lead to a more general conclusion. Fast-walking insects appear to be confronted with optical requirements that are similar to those of many flying insects, whose optical environment is dominated by fast optic flow parallel to the longitudinal axis of the body and slow optic flow in the vertical direction (hence the horizontal extension and vertical compression of $\Delta\varphi$; Land, 1989).

There remains the question of how the overall shape of the compound eye changes with increasing head width and how these changes are related to the optical spacing of the ommatidial axes. First, it appears that, in workers of different sizes, the directions of the optical axes of the ommatidia (expressed in spherical coordinates) map onto corresponding positions on the compound eye (expressed in ommatidial row coordinates; Fig. 4A). This signifies that not only the boundaries of the visual field but also the spatial distribution of the optical axes as a whole remain constant. Thus, one might expect that the shape of the surface of the compound eye would be similar in individuals of different sizes. Surface data sampled along a line leading from the upper to the lower margin of the compound eye (Fig. 6) show that the radius of curvature exhibits a characteristic pattern of zonal variation that is identical for small and large individuals. Moreover, the total length of the curved segment (D_{75}) as well as the mean radius of curvature (R_c) scale nearly linearly with head width (Table 2). The straight-line distance between the upper and lower margins of the compound eye (H_c, eye height) also scales linearly with head width. This suggests that the overall shape of the compound eye surface remains constant, which may be an important morphological prerequisite for the optical mapping properties described above.

References

AUTRUM, H. AND WIEDEMANN, J. (1962). Versuche über den Strahlengang im Insektenauge. *Z. Naturforsch.* **17b**, 480–482.

BARLOW, H. B. (1952). The size of ommatidia in apposition eyes. *J. exp. Biol.* **29**, 667–674.

BAUMGÄRTNER, H. (1928). Der Formensinn und die Sehschärfe der Bienen. *Z. vergl. Physiol.* **7**, 56–143.

DEL PORTILLO, J. (1936). Beziehungen zwischen den Oeffnungswinkeln der Ommatidien, Krümmung und Gestalt der Insekten-Augen und ihrer funktionellen Aufgabe. *Z. vergl. Physiol.* **23**, 100–145.

FENT, K. (1985). Himmelsorientierung bei der Wüstenameise *Cataglyphis bicolor*: Bedeutung von Komplexaugen und Ocellen. PhD thesis, University of Zürich.

FRANCESCHINI, N. (1975). Sampling of the visual environment by the compound eye of the fly: fundamentals and applications. In

Photoreceptor Optics (ed. A. W. Snyder and R. Menzel), pp. 97–125. Berlin, Heidelberg, New York: Springer.

FRANKS, N. R. AND NORRIS, P. J. (1987). Constraints on the division of labour in ants: D'Arcy Thompson's Cartesian transformations applied to worker polymorphism. In *Behavior in Social Insects*, *Experientia* (Supplement), vol. **54** (ed. J. M. Pasteels and J.-L. Deneubourg), pp. 253–270. Basel, Boston: Birkhäuser.

HÖLLDOBLER, B. AND WILSON, E. O. (1990). *The Ants*. Cambridge, MA: Belknap Press of Harvard University Press.

HORRIDGE, G. A. (1978). The separation of visual axes in apposition compound eyes. *Phil. Trans. R. Soc. Lond. B* **285**, 1–59.

KIRSCHFELD, K. (1976). The resolution of lens and compound eyes. In *Neural Principles in Vision* (ed. F. Zettler and R. Weiler), pp. 354–370. Berlin, Heidelberg, New York: Springer.

LAND, M. F. (1981). Optics and vision in invertebrates. In *Handbook of Sensory Physiology*, vol. VII/6B (ed. H. Autrum), pp. 471–592. Berlin, Heidelberg, New York: Springer.

LAND, M. F. (1989). Variations in the structure and design of compound eyes. In *Facets of Vision* (ed. D. G. Stavenga and R. C. Hardie), pp. 90–11. Berlin, Heidelberg, New York: Springer.

MENZEL, R. AND WEHNER, R. (1970). Augenstrukturen bei verschieden grossen Arbeiterinnen von *Cataglyphis bicolor* Fabr. *Z. vergl. Physiol.* **68**, 446–449.

SNYDER, A. W. (1979). Physics of vision in compound eyes. In *Handbook of Sensory Physiology*, vol. VII/6A (ed. H. Autrum), pp. 225–313. Berlin, Heidelberg, New York: Springer.

STAVENGA, D. G. (1979). Pseudopupils of compound eyes. In *Handbook of Sensory Physiology*, vol. VII/6A (ed. H. Autrum), pp. 357–439. Berlin, Heidelberg, New York: Springer.

STAVENGA, D. G. (1992). Eye regionalization and spectral tuning of retinal pigments in insects. *Trends Neurosci.* **15**, 213–217.

VIA, S. E. (1977). Visually mediated snapping in the bulldog ant: a perceptual ambiguity between size and distance. *J. comp. Physiol.* **121**, 33–51.

WEHNER, R. (1981). Spatial vision in arthropods. In *Handbook of Sensory Physiology*, vol. VII/6C (ed. H. Autrum), pp. 287–616. Berlin, Heidelberg, New York: Springer.

WEHNER, R. (1983). Taxonomie, Funktionsmorphologie und Zoogeographie der saharischen Wüstenameise *Cataglyphis fortis* (Forel 1902) stat. nov. (Insecta: Hymenoptera: Formicidae). *Senckenbergiana biol.* **64**, 89–132.

WEHNER, R. (1987). Spatial organization of foraging behavior in individually searching ants, *Cataglyphis* (Sahara desert) and *Ocymyrmex* (Namib desert). In *Behavior in Social Insects*, *Experientia* (Supplement), vol. **54** (ed. J. M. Pasteels and J.-L. Deneubourg), pp. 15–42. Basel, Boston: Birkhäuser.

WEHNER, R. (1991). Highly parallel processing in the visual system of an insect's brain (*Cataglyphis bicolor*). *Proc. Neurobiol. Conf. Göttingen* **19**, 270.

WEHNER, R. (1992). Arthropods. In *Animal Homing* (ed. F. Papi), pp. 45–144. London: Chapman and Hall.

WEHNER, R. (1994). The polarization-vision project: championing organismic biology. In *Neural Basis of Behavioural Adaptation* (ed. K. Schildberger and N. Elsner), pp. 103–143. Stuttgart, New York: G. Fischer.

WEHNER, R., BRUNNERT, A., HERRLING, P. L. AND KLEIN, R. (1972). Periphere Adaption und zentralnervöse Umstimmung im optischen System von *Cataglyphis bicolor* (Formicidae, Hymenoptera). *Rev. suisse Zool.* **79**, 197–228.

WEHNER, R., WEHNER, S. AND AGOSTI, D. (1994). Patterns of biogeographical distribution within the *bicolor* group of the North African desert ant *Cataglyphis* Foerster 1850 (Insecta: Hymenoptera: Formicidae). *Senckenbergiana biol.* **74**, 163–191.

ZOLLIKOFER, C. P. E. (1994). Stepping patterns in ants. III. Influence of body size. *J. exp. Biol.* **192**, 107–118.